JOC Article

Emission from Regioisomeric Bis(phenylethynyl)benzenes during Pulse Radiolysis

Shingo Samori, Sachiko Tojo, Mamoru Fujitsuka, Torben Ryhding,[†] Aaron G. Fix,[†] Brittany M. Armstrong,[†] Michael M. Haley,[†] and Tetsuro Majima*

The Institute of Scientific and Industrial Research (SANKEN), Osaka University, Mihogaoka 8-1, Ibaraki, Osaka 567-0047, Japan, and Department of Chemistry and the Materials Science Institute, University of Oregon, Eugene, Oregon 97403-1253

majima@sanken.osaka-u.ac.jp

Received March 5, 2009

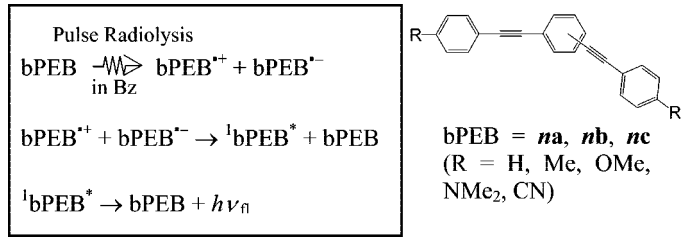

Emission from charge recombination between radical cations and anions of a series of regioisomeric 1,4-, 1,3-, and 1,2-bis(phenylethynyl)benzenes (bPEBs) substituted by various electron donor and/or acceptor groups was measured during pulse radiolysis in benzene (Bz). The formation of bPEB in the excited singlet state (^{1}bPEB*) can be attributed to the charge recombination between bPEB$^{\bullet+}$ and bPEB$^{\bullet-}$, which are initially generated from the radiolytic reaction. This mechanism is reasonably explained by the relationship between the annihilation enthalpy change ($-\Delta H°$) for the charge recombination of bPEB$^{\bullet+}$ and bPEB$^{\bullet-}$ and excitation energy of ^{1}bPEB*. Since the degree of the π-conjugation in the S_1 state and HOMO−LUMO levels of bPEB change with the substitution pattern of phenylacetylene groups on the central benzene ring and the various kinds of donor and/or acceptor group, the fine-tuning of the emission color and intensity of bPEB can be easily carried out during pulse radiolysis in Bz. For donor-acceptor-substituted bPEB, it was found that the difference in the charge transfer conjugated pathways between donor and acceptor substituents (linear-, cross-, and "bent"-conjugated pathways) strongly influenced the HOMO−LUMO energy gap.

Introduction

Electron detachment from and attachment to a solute molecule (M) generates a radical cation (M$^{\bullet+}$) and anion (M$^{\bullet-}$), respectively. M$^{\bullet+}$ and M$^{\bullet-}$ are known as important ionic intermediates in photochemistry, electrochemistry, and radiation chemistry.[1] It is well-known that M in the excited states (M* = ^{1}M* (excited singlet state) and ^{3}M* (excited triplet state)) can be formed by charge recombination between M$^{\bullet+}$ and M$^{\bullet-}$ (M$^{\bullet+}$ + M$^{\bullet-}$ → M* + M), after which ^{1}M* deactivates to M in the ground-state by emitting light (^{1}M* → M + $h\nu_{fl}$).[2] This process is significant for optoelectronic materials such as OLEDs because electrochemical energies can be converted to photochemical energies.

Recently, we have found that various π-conjugated compounds showed emission during pulse radiolysis in benzene (Bz).[3] In pulse radiolysis of M in Bz, the ionization of Bz to

[†] University of Oregon.

(1) (a) Fox, M. A.; Chanon, M. *Photoinduced Electron Transfer*; Elsevier: Amsterdam, 1988. (b) Kavarnos, G. J.; Turro, N. J. *Chem. Rev.* **1986**, *86*, 401.

(2) (a) Faulkner, L. R.; Bard, A. J. *Electroanalytical Chemistry*; Marcel Dekker: New York, 1977; Vol. 10, pp 1−95. (b) Bard, A. J.; Faulkner, L. R. *Electrochemical Methods Fundamentals and Applications*, 2nd ed.; John Wiley and Sons: New York, 2001; pp 736−745. (c) Richter, M. M. *Chem. Rev.* **2004**, *104*, 3003.

(3) (a) Samori, S.; Hara, M.; Tojo, S.; Fujitsuka, M.; Yang, S.-W.; Elangovan, A.; Ho, T.-I.; Majima, T. *J. Phys. Chem. B* **2005**, *109*, 11735. (b) Samori, S.; Tojo, S.; Fujitsuka, M.; Yang, S.-W.; Elangovan, A.; Ho, T.-I.; Majima, T. *J. Org. Chem.* **2005**, *70*, 6661. (c) Samori, S.; Tojo, S.; Fujitsuka, M.; Yang, S.-W.; Ho, T.-I.; Yang, J.-S.; Majima, T. *J. Phys. Chem. B* **2006**, *110*, 13296. (d) Samori, S.; Tojo, S.; Fujitsuka, M.; Liang, H.-J.; Ho, T.-I.; Yang, J.-S.; Yang, S.-W.; Majima, T. *J. Org. Chem.* **2006**, *71*, 8732. (e) Samori, S.; Tojo, S.; Fujitsuka, M.; Lin, J.-H.; Ho, T.-I.; Yang, J.-S.; Majima, T. *J. Chin. Chem. Soc.* **2006**, *53*, 1225. (f) Samori, S.; Tojo, S.; Fujitsuka, M.; Splitler, E. L.; Haley, M. M.; Majima, T. *J. Org. Chem.* **2007**, *72*, 2785. (g) Samori, S.; Tojo, S.; Fujitsuka, M.; Splitler, E. L.; Haley, M. M.; Majima, T. *J. Org. Chem.* **2008**, *73*, 3551.

10.1021/jo900494j CCC: $40.75
Published on Web 04/14/2009

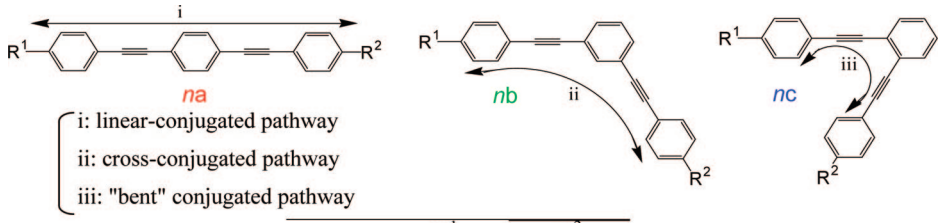

n	R^1	R^2
1	H	H
2	Me	H
3	OMe	H
4	CN	H
5	Me	CN
6	OMe	CN
7	NMe_2	CN

FIGURE 1. Chemical structures of bis(phenylethynyl)benzene derivatives (bPEBs). Arrows (i−iii) show three types of charge transfer conjugated pathways in bPEBs.

give Bz radical cation ($Bz^{\bullet+}$) and formation of an electron (e^-) occur at the same time, followed by reaction with M to give $M^{\bullet+}$ and $M^{\bullet-}$, respectively. In our previous work, we have proposed that the charge recombination of $M^{\bullet+}$ and $M^{\bullet-}$ gives $^1M^*$ and/or $^1M_2^*$ as the emissive species for the organic electrochemiluminescent molecules such as phenylquinolinylethynes,[3a] phenyl(9-acridinyl)ethynes,[3b] phenyl(9-cyanoanthracenyl)-ethynes,[3b,d] arylethynylpyrenes,[3c] 9-cyano-10-(*p*-substituted phenyl)anthracenes,[3e] and 1,2,4,5-tetrakis(arylethynyl)benzenes (TAEBs).[3f,g]

For optoelectronic applications, organic compounds possessing a high degree of π-conjugation with donor and/or acceptor groups have been recognized as ideal materials.[4−6] Changes in the substituents and substitution pattern, electronic structure, and conjugation can provide highly variable photophysical properties for such materials. As a class of π-conjugated molecules with remarkable optoelectronic properties, functionalized phenylacetylene structures have received considerable attention because of their characteristic conjugated pathways.[6−8] In particular, 1,4-, 1,3-, and 1,2-bis(phenylethynyl)benzenes (bPEBs = ***n*a**, ***n*b**, and ***n*c**) containing both donor and acceptor functionality are an ideal class of molecules for studying the differences between the linear- (path i), cross- (path ii), and "bent"-conjugated (path iii) pathways to gain a better understanding of the geometric aspects of the charge-transfer pathways (Figure 1). By varying the substitution pattern of the donor- or acceptor-substituted phenylacetylene group at the central benzene ring, each charge-transfer pathway can be modified. Therefore, the donor-acceptor-type bPEB structures can avoid the complexity of the charge transfer pathways observed in TAEB structures having two-donor and two-acceptor groups. In addition, the HOMO−LUMO energy gaps of neutral **1a** and **1c** have been reported to be 7.043 and 6.874 eV, respectively, which are much lower than that of **1b** (7.338 eV).[9] This feature indicates that the emission wavelength of the bPEB structure dramatically changes with the different types of branching. Consequently, we can easily fine-tune the emission wavelength and intensity by changing the various types of donor and acceptor substituents and the substitution pattern of the central arene. Some of these compounds are expected to be useful for OLED materials because of the sufficiently large fluorescent quantum yield (Φ_{fl}) and excess energy value ($-\Delta H^\circ - E_{S1}$) (details are discussed below). In addition, bPEB structures can rotate freely about their C−C single bonds,[3f,g] decreasing π-orbital overlap, and thus formation of the face-to-face excimer structure with less luminescence intensity cannot be expected. The time-resolved transient absorption and emission measurements during the pulse radiolysis of various bPEBs are useful

(4) (a) Goes, M.; Verhoeven, J. W.; Hofstraat, H.; Brunner, K. *ChemPhysChem* **2003**, *4*, 349. (b) Thomas, K. R. J.; Lin, J. T.; Tao, Y.-T.; Chuen, C.-H. *Chem. Mater.* **2002**, *14*, 3852. (c) Zhu, W.; Hu, M.; Yao, R.; Tian, H. *J. Photochem. Photobiol., A* **2003**, *154*, 169. (d) Thomas, K. R. J.; Lin, J. T.; Velusamy, M.; Tao, Y.-T.; Chuen, C.-H. *Adv. Funct. Mater.* **2004**, *14*, 83. (e) Chiang, C.-L.; Wu, M.-F.; Dai, D.-C.; Wen, Y.-S.; Wang, J.-K.; Chen, C.-T. *Adv. Funct. Mater.* **2005**, *15*, 231.

(5) (a) Elangovan, A.; Chen, T.-Y.; Chen, C.-Y.; Ho, T.-I. *Chem. Commun.* **2003**, 2146. (b) Elangovan, A.; Yang, S.-W.; Lin, J.-H.; Kao, K.-M.; Ho, T.-I. *Org. Biomol. Chem.* **2004**, *2*, 1597. (c) Elangovan, A.; Chiu, H.-H.; Yang, S.-W.; Ho, T.-I. *Org. Biomol. Chem.* **2004**, *2*, 3113. (d) Elangovan, A.; Kao, K.-M.; Yang, S.-W.; Chen, Y.-L.; Ho, T.-I.; Su, Y. O. *J. Org. Chem.* **2005**, *70*, 4460. (e) Yang, S.-W.; Elangovan, A.; Hwang, K.-C.; Ho, T.-I. *J. Phys. Chem. B* **2005**, *109*, 16628. (f) Lin, J.-H.; Elangovan, A.; Ho, T.-I. *J. Org. Chem.* **2005**, *70*, 7397.

(6) (a) Jayakannan, M.; Van Hal, P. A.; Janssen, R. A. J. *J. Polym. Sci., Part A: Polym. Chem.* **2001**, *40*, 251. (b) Tykwinski, R. R.; Schreiber, M.; Carlon, R. P.; Diederich, F.; Gramlich, V. *Helv. Chim. Acta* **1996**, *79*, 2249. (c) Tykwinski, R. R.; Schreiber, M.; Gramlich, V.; Seiler, P.; Diederich, F. *Adv. Mater.* **1996**, *8*, 226. (d) Wilson, J. N.; Hardcastle, K. I.; Josowicz, M.; Bunz, U. H. F. *Tetrahedron* **2004**, *60*, 7157. (e) Wilson, J. N.; Smith, M. D.; Enkelmann, V.; Bunz, U. H. F. *Chem. Commun.* **2004**, 1700. (f) Wilson, J. N.; Josowicz, M.; Wang, Y.; Bunz, U. H. F. *Chem. Commun.* **2003**, 2962. (g) Miteva, T.; Palmer, L.; Kloppenburg, L.; Neher, D.; Bunz, U. H. F. *Macromolecules* **2000**, *33*, 652. (h) J. Zucchero, A.; Wilson, J. N.; Bunz, U. H. F. *J. Am. Chem. Soc.* **2006**, *128*, 11872. (i) Ojima, J.; Kakumi, H.; Kitatani, K.; Wada, K.; Ejiri, E.; Nakada, T. *Can. J. Chem.* **1984**, *63*, 2885. (j) Ojima, J.; Enkaku, M.; Uwai, C. *Bull. Chem. Soc. Jpn.* **1977**, *50*, 933.

(7) (a) Miller, J. J.; Marsden, J. A.; Haley, M. M. *Synlett* **2004**, 165. (b) Marsden, J. A.; Miller, J. J.; Shirtcliff, L. D.; Haley, M. M. *J. Am. Chem. Soc.* **2005**, *127*, 2464. (c) Spitler, E. L.; Shirtcliff, L. D.; Haley, M. M. *J. Org. Chem.* **2007**, *72*, 86. (d) Spitler, E. L.; Monson, J. M.; Haley, M. M. *J. Org. Chem.* **2008**, *73*, 2211.

(8) (a) Marsden, J. A.; Palmer, G. J.; Haley, M. M. *Eur. J. Org. Chem.* **2003**, 2355. (b) Jones, C. S.; O'Connor, M. J.; Haley, M. M. In *Acetylene Chemistry: Chemistry, Biology, and Materials Science*; Diederich, F., Tykwinski, R. R., Stang, P. J., Eds.; Wiley-VCH: Weinheim, Germany, 2004; pp 303−385. (c) Marsden, J. A.; Haley, M. M. *J. Org. Chem.* **2005**, *70*, 10213. (d) Anand, S.; Varnavski, O.; Marsden, J. A.; Haley, M. M.; Schlegel, H. B.; Goodson, T., III. *J. Phys. Chem. A* **2006**, *110*, 1305. (e) Bhaskar, A.; Guda, R.; Haley, M. M.; Goodson, T., III. *J. Am. Chem. Soc.* **2006**, *128*, 13972. (f) Slepkov, A. D.; Hegmann, F. A.; Tykwinski, R. R.; Kamada, K.; Ohta, K.; Marsden, J. A.; Spitler, E. L.; Miller, J. J.; Haley, M. M. *Opt. Lett.* **2006**, *31*, 3315. (g) Spitler, E. L.; McClintock, S. P.; Haley, M. M. *J. Org. Chem.* **2007**, *72*, 6692.

(9) Zhang, W.; Huang, C. *Mater. Chem. Phys.* **2006**, *96*, 283.

SCHEME 1. Synthesis of bPEB 6c

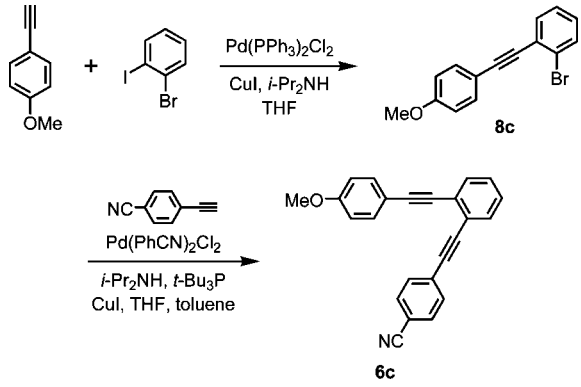

to gain a better understanding of the emission mechanism, providing valuable information for molecular design with efficient luminescence character.

In this paper, we report the emission from the charge recombination bPEB$^{\bullet+}$ and bPEB$^{\bullet-}$ of 21 different bPEB derivatives (***n*a**, ***n*b**, and ***n*c**; $n = 1-7$): nonsubstituted (**1a**−**c**), methyl-substituted (**2a**−**c**), methoxy-substituted (**3a**−**c**), cyano-substituted (**4a**−**c**), methyl- and cyano-substituted (**5a**−**c**), methoxy- and cyano-substituted (**6a**−**c**), and dimethylamino- and cyano-substituted bPEBs (**7a**−**c**). When *n* is the same, 1,4- (***n*a**), 1,3- (***n*b**), and 1,2-bPEBs (***n*c**) are regioisomers (Figure 1). The detailed study of 21 different kinds of bPEBs potentially leads to customization of optical band gaps and luminescent efficiency for specialized materials applications.

Results and Discussion

Synthesis. Of the 21 bPEBs in this study, compounds **1a**−**c**,[10] **2a**,[11] **3a**−**c**,[12] **4a**,[13] **6a**,[14] and **7a**[14] have been previously described in the literature. The other 11 bPEB structures were synthesized by sequential Sonogashira reactions using 1,2-, 1,3-, or 1,4-bromoiodobenzene as the core arene, illustrated for **6c** in Scheme 1. Cross-coupling 4-ethynylanisole to 1-bromo-2-iodobenzene afforded bromoarene **8c**. This was in turn cross-coupled to 4-ethynylbenzonitrile using the more reactive catalytic system $PdCl_2(PhCN)_2/t$-Bu_3P first reported by Buchwald and Fu,[15] furnishing bPEB **6c** in 36% yield for the two steps. The remaining 10 bPEBs were prepared analogously in ca. 20−40% unoptimized yield (see Supporting Information).

Steady-State Spectral Properties of bPEB. Normalized steady-state absorption and fluorescence spectra of bPEB in Bz are shown in Figure 2. It seems that the electronic structures of bPEB strongly depend on the substitution pattern of the phenylacetylene group because the regioisomers (*ortho*-, *meta*-, and *para*-substituted isomers) have similar spectral shapes. It is well-known that the *meta* branching type **1b** disrupts the

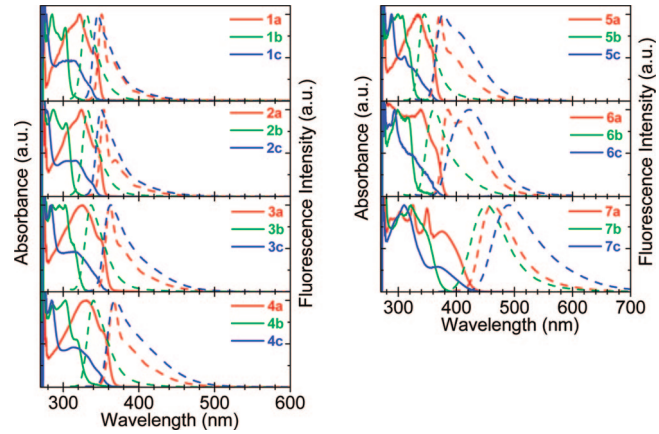

FIGURE 2. Absorption (solid lines) and fluorescence (broken lines) spectra observed by the steady-state measurement of bPEB in Ar-saturated Bz. All solutions were prepared at a dilute concentration (10^{-5} M).

TABLE 1. Emission Properties of bPEB in Ar-Saturated Bz

	a		b		c	
bPEB	λ^{Fl} (nm)	Φ_{fl}	λ^{Fl} (nm)	Φ_{fl}	λ^{Fl} (nm)	Φ_{fl}
1	351	0.90	331	0.25	346	0.34
2	354	0.93	332	0.22	350	0.44
3	362	0.82	337	0.065	363	0.63
4	367	0.93	340	0.54	369	0.61
5	372	0.99	345	0.63	377	0.60
6	386	0.85	361	0.63	422	0.50
7	462	0.39	452	0.29	490	0.34

π-conjugation; thus, the absorption spectra of **1b** is predicted to resemble the absorption spectrum of diphenylacetylene (DPA).[16] A comparison of the absorption spectra of DPA and **1b** show that, indeed, this is the case: the spectrum of **1b** reproduces the spectral width and vibronic structure displayed by DPA. In contrast, when substitution occurs at the *para* position (**1a**), the absorption band edge is red-shifted by 30 nm with respect the band edge of **1b** and appears at 355 nm. The relatively large red shift and loss of the sharp vibronic structure reflect the π-electron delocalization over the linear three-ring chain. The *ortho* branching type **1c** exhibits an absorption band edge at 350 nm, which confirms that π-electron delocalization occurs over the bent three-ring chain, although the red shift is somewhat smaller than that of **1a**. Compared to neutral **1**, donor types **2** and **3**, and acceptor type **4**, the corresponding absorption bands of donor-acceptor-substituted bPEBs **5**−**7** are broadened and show further bathochromic shifts, indicating the intramolecular charge transfer (ICT) from the donor to the acceptor for the HOMO−LUMO transition.[7]

Fluorescence was observed for all bPEBs (Figure 2). Compared to neutral **1**, donor-acceptor types **5**−**7** showed a large red shift in the fluorescence maxima in Bz. This again indicates ICT character for donor-acceptor-substituted bPEB in the S_1 state (Table 1). **5**−**7** showed strong fluorescence solvatochromism, experiencing bathochromic shifts in switching to a more polar solvent such as CH_3CN. This also indicates the ICT character for the donor-acceptor-substituted bPEBs in the S_1 state. It should be noted that the fluorescence maxima of neutral **1** increase in the order **1b** (331 nm) < **1c** (346 nm) < **1a** (351 nm), whereas those of donor-acceptor-type **7** increase in the

(10) (a) Nguyen, P.; Yuan, Z.; Agocs, L.; Lesley, G.; Marder, T. B. *Inorg. Chem. Acta* **1994**, *220*, 289. (b) Songkram, C.; Takaishi, K.; Yamaguchi, K.; Kagechika, H.; Endo, Y. *Tetrahedron Lett.* **2001**, *42*, 6365. (c) Kovalenko, S. V.; Peabody, S.; Manoharan, M.; Clark, R. J.; Alabugin, I. V. *Org. Lett.* **2004**, *6*, 2457.

(11) Drefahl, G.; Plotner, G. *Chem. Ber.* **1958**, *91*, 1280. This compound was originally prepared by stilbene bromination/dehydrobromination. An improved preparation via Sonogashira reactions as well as NMR spectroscopic data are given in Supporting Information.

(12) Ye, F.; Orita, A.; Doumoto, A.; Otera, J. *Tetrahedron* **2003**, *59*, 5635.

(13) Dirk, S. M.; Tour, J. M. *Tetrahedron* **2003**, *59*, 287.

(14) Nguyen, P.; Lesley, G.; Marder, T. B.; Ledoux, I.; Zyss, J. *Chem. Mater.* **1997**, *9*, 406.

(15) Hundertmark, T.; Littke, A. F.; Buchwald, S. L.; Fu, G. C. *Org. Lett.* **2000**, *2*, 1729.

(16) Melinger, J. S.; Pan, Y.; Kleiman, V. D.; Peng, Z.; Davis, B. L.; McMorrow, D.; Lu, M *J. Am. Chem. Soc.* **2002**, *124*, 12002.

order **7b** (452 nm) < **7a** (462 nm) < **7c** (490 nm). This result clearly indicates that the bent-conjugated charge transfer pathway (path iii) leads the fluorescence band to longer wavelength than the linear-conjugated charge transfer pathway (path i). Compared to cross- (path ii) and bent-conjugated (path iii) charge transfer pathways, it seems that the linear-conjugated charge transfer pathway (path i) leads a slight red shift when bPEB has both donor and acceptor substituents. Consequently, it is clearly evident that the difference in the charge transfer conjugated pathways between donor and acceptor substituents strongly influences the HOMO−LUMO energy gap, although we cannot clearly investigate this because of the complexity of the charge transfer pathways observed in TAEB structures in our previous reports.[3f,g,7,8]

The fluorescence quantum yield (Φ_{fl}) values of the bPEBs ranged from 0.065 to 0.99 and showed the tendency for *para* (0.39−0.99), *ortho* (0.34−0.63), and *meta* isomers (0.065−0.63), in decreasing order. Recently, it was reported that there was a correlation between the Φ_{fl} and the magnitude (A_π) of the π-conjugation length in the excited singlet state for various π-conjugated hydrocarbons including **1a**, **1b**, and nonsubstituted TAEB.[17] The relationship between Φ_{fl} and A_π is expressed by the following simple equation:

$$\Phi_{fl} = \frac{1}{\exp(-A_\pi)} + 1 \qquad (1)$$

As mentioned above, the *meta* branching disrupts the π-electron conjugation; thus, the A_π value of ***n*b** should be smaller than those of ***n*a** and ***n*c**. The lower Φ_{fl} value of ***n*b** can be reasonably explained by eq 1. On the other hand, for the *para* type ***n*a**, the π-electrons are delocalized over the whole molecule, indicating the A_π value of ***n*a** should be larger than those of the others. Although the π-electron delocalization also occurs in *ortho* type ***n*c**, the degree of the π-conjugation is assumed to be smaller than ***n*a**. As a result, the Φ_{fl} value of ***n*c** is midway between those of ***n*a** and ***n*b**. The lower Φ_{fl} value of **7** compared with the others can be explained by the energy-gap law.[18] From the intersection point of the absorption and fluorescence spectra, the excitation energies of **7a**, **7b**, and **7c** (E_{S1} = 2.94, 3.18, and 2.88 eV, respectively) are estimated to be smaller than those of other bPEBs (3.33−3.97 eV). The increase of internal conversion rate is expected and responsible for the low Φ_{fl} values of **7**. The Φ_{fl} value of **3b** is exceptionally low (0.065). Methoxy groups are not known to quench fluorescence in fluorescent molecules, such as in stilbenes,[19a] coumarins,[19b,c] quinolinones,[19c] and fluoranthenes.[19d] The reason for the strong fluorescence quenching of **3b** is still unclear.

Emission Generated from Charge Recombination between bPEB$^{\bullet+}$ and bPEB$^{\bullet-}$. Emission spectra were observed after an electron pulse during the pulse radiolysis of bPEB in Ar-saturated Bz (1.0 mM) (Figure 3). According to previous reports,[3] the emission of M indicates the generation of ^{1}M* by charge recombination of M$^{\bullet+}$ and M$^{\bullet-}$ during pulse radiolysis in Bz. When N_2O gas was added to the solution as the electron scavenger, the emission intensity observed during the pulse radiolysis of bPEB in Bz was reduced. This result clearly indicates that bPEB$^{\bullet+}$ and bPEB$^{\bullet-}$ are responsible to the emission during the pulse radiolysis. The same emission mechanism was assumed for bPEB as shown the following (Scheme 2).

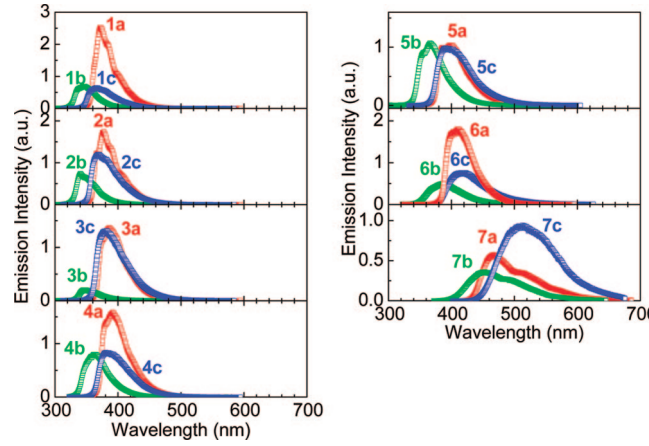

FIGURE 3. Emission spectra observed in the time range of 0−100 ns during pulse radiolysis of bPEB in Ar-saturated Bz (10^{-3} M).

SCHEME 2. Proposed Mechanism of the Emission during the Pulse Radiolysis of bPEB in Bz[a]

$$Bz \rightsquigarrow e^- + Bz^{\bullet+}$$

$$Bz^{\bullet+} + e^- \rightarrow Bz^*$$

$$Bz^{\bullet+} + bPEB \rightarrow bPEB^{\bullet+}$$

$$e^- + bPEB \rightarrow bPEB^{\bullet-}$$

$$bPEB^{\bullet+} + bPEB^{\bullet-} \rightarrow {}^1bPEB^* + bPEB \text{ and } {}^3bPEB^* + bPEB \quad \text{(within pulse duration (8 ns))}$$

$$^1bPEB^* \rightarrow bPEB + h\nu_{fl}\ (\tau_{fl} < 8\ ns)$$

[a] For donor-acceptor-substituted bPEBs (**5**−**7**), ^{1}bPEB* = ^{1}(A$^{\bullet-}$ − D$^{\bullet+}$)* (ICT state).

Little or no emission was observed during the pulse radiolysis of bPEB in 1,2-dichloroethane (DCE) or *N*,*N*-dimethylformamide (DMF), indicating that bPEB$^{\bullet+}$ and bPEB$^{\bullet-}$ do not emit light. In other words, both bPEB$^{\bullet+}$ and bPEB$^{\bullet-}$ must be formed at the same time in order to emit light. In Bz, no transient absorption band of bPEB$^{\bullet+}$ and bPEB$^{\bullet-}$ was observed immediately after an 8 ns electron pulse. Therefore, it is assumed that bPEB$^{\bullet+}$ and bPEB$^{\bullet-}$ immediately recombine to give ^{1}bPEB* and ^{3}bPEB*, and ^{1}bPEB* emits light within a pulse duration. The transient absorption spectra observed during the pulse radiolysis of bPEB in Ar-saturated Bz can be assigned to ^{3}bPEB* (triplet−triplet absorption).

Because of the considerable repulsion between the substituents induced by the rotation around C−C single bonds, a π-stacked structure cannot be formed for the interaction between bPEB$^{\bullet+}$ and bPEB$^{\bullet-}$. Therefore, bPEB showed only monomer emission, although some electrochemiluminescent molecules showed both monomer and excimer emissions with less luminescence intensity during pulse radiolysis as mentioned in previous reports.[3]

Compounds **1**−**7** showed emission peaks at 373−513 nm during the pulse radiolysis (Figures 2). The shape of the emission spectra of bPEB was similar to those observed in the steady-state measurements, although the emission spectra of bPEB were

(17) Yamaguchi, Y.; Matsubara, Y.; Ochi, T.; Wakamiya, T.; Yoshida, Z. *J. Am. Chem. Soc.* **2008**, *130*, 13867.
(18) Kasha, M. *Chem. Rev.* **1947**, *41*, 401.
(19) (a) Roberts, J. C.; Pincock, J. A. *J. Org. Chem.* **2006**, *71*, 1480. (b) Mateera, N. N.; Kode, R. A.; Redda, K. K. *J. Heterocycl. Chem.* **2002**, *39*, 1251. (c) Charitos, C.; Tzougraki, C.; Kokotos, G. *J. Peptide Res.* **2000**, *56*, 373. (d) Tucker, S. A.; Griffin, J. M.; Acree, W. E., Jr.; Tanga, M. J.; Bupp, J. E.; Tochimoto, T. K.; Lugtenburg, J. A.; Van Haeringen, K.; Cornelisse, J. *Polycyclic Aromat. Compd.* **1994**, *4*, 161.

TABLE 2. Emission Maxima (λ_{max}^{Em}) and Relative Emission Intensities (I) during Pulse Radiolysis of bPEB in Ar-Saturated Bz (1.0 mM)

	a		b		c	
bPEB	λ_{max}^{Em} (nm)	I^a	λ_{max}^{Em} (nm)	I	λ_{max}^{Em} (nm)	I
1	373	100	348	35.2	365	35.0
2	378	73.5	341	34.0	368	64.3
3	386	64.6	348	9.92	382	71.0
4	392	74.1	361	42.5	381	46.5
5	398	53.1	366	57.7	391	59.0
6	409	85.0	386	31.1	421	45.6
7	467	30.4	453	23.9	513	56.4

[a] I values of bPEB were determined from the total amount of the emission spectra observed during pulse radiolysis, relative to I value of **1a** in Ar-saturated Bz.

observed at the slightly longer wavelength due to the self-absorption as a result of the high concentrations.[3] Therefore, the formation of ^{1}bPEB* with ICT character can be assumed for **5**−**7** during pulse radiolysis. The intensities (I) of the radiolysis-induced emission spectra of **1**−**7** were determined from the total amount of the emission observed during pulse radiolysis and are summarized in Tables 2.

To elucidate the emission mechanism of the bPEBs, we estimated the annihilation enthalpy change ($-\Delta H°$) value for the charge recombination between $M^{\bullet+}$ and $M^{\bullet-}$. This $-\Delta H°$ value is a criterion for whether ^{1}M* can be formed by the charge recombination or not.[2] $-\Delta H°$ is calculated by eq 2:[20]

$$-\Delta H° = (E_{ox} - E_{red})^{\varepsilon_s} - \Delta G_{sol}{}^{\varepsilon_s} - w_{a,\mu} + T\Delta S° \qquad (2)$$

where E_{ox} and E_{red} are the oxidation and reduction potentials of M, respectively. ε_s, ΔG_{sol}, and $w_{a,\mu}$ represent the static dielectric constant of solvent, the free energy change of solvation, and the work required to bring $M^{\bullet+}$ and $M^{\bullet-}$ within a likely separation distance, respectively. For bPEB in Bz, $-\Delta H°$ can be expressed using E_{ox} and E_{red} measured in CH_3CN by simplified eq 3:[3]

$$-\Delta H° = E_{ox} - E_{red} + 0.19\text{eV} \qquad (3)$$

The calculated $-\Delta H°$ values for bPEB are listed in Table 3, together with their oxidation and reduction potentials and E_{S1} values. $-\Delta H°$ values for all bPEBs (3.05−4.36 eV) are consistently larger than their E_{S1} values (2.88−3.97 eV), indicating that the energy available in the charge recombination is sufficient to populate all bPEBs in the S_1 states.

As shown in Figure 4, the I value seems proportional to Φ_{fl}. However, the I value of some bPEBs deviates from the fitted line. The decrease of the I value was explained by the self-absorption. In our previous paper,[3] the energy differences between $-\Delta H°$ and E_{S1} ($-\Delta H° - E_{S1}$ (= +0.01−0.61 eV)) were also assumed as one of the key factors for the I value of Ms. Therefore, these deviated plots are assumed to depend on not only Φ_{fl} and the amount of the self-absorption but also the ($-\Delta H° - E_{S1}$) value.

Fine-Tuning of the Emission Color and Intensity by Changing the Substitution Pattern of Donor-Acceptor-Subsituted bPEB. Donor-acceptor-substituted bPEBs ***n*a**, ***n*b**, and ***n*c** (n = 5−7) can contain the conjugated pathways: linear- (path i), cross- (path ii), and bent-conjugated (path iii) pathways, respectively, as shown in Figure 1. The emission spectra of ^{1}bPEB* with ICT character depends on the substitution pattern by the steady-state measurement and during the pulse radiolysis as shown in Figures 2 and 3, respectively. The radiolysis-induced emission spectra of all bPEBs showed emission bands in the region of wavelength where the fluorescence bands were observed by the steady-state measurements. For **5**−**7**, therefore, the charge recombination between $bPEB^{\bullet+}$ and $bPEB^{\bullet-}$ generates ^{1}bPEB* with ICT character as shown in Scheme 3. The results also indicate that the difference in the charge transfer conjugated pathways strongly influences the HOMO−LUMO energy gap: the bent-conjugated charge transfer pathway (path iii) leads the fluorescence band to longer wavelength than the linear- (path i) and cross-conjugated (path ii) charge transfer pathways when bPEB has both donor and acceptor substituents. Consequently, it is evident that judicious choice of the donor/acceptor unit permits control of the HOMO−LUMO energy gap, and thus the emission wavelengths can be fine-tuned at around 450−650 nm in the visible region.

As shown in Table 2, the I values of ***n*b** are lower than those of ***n*a** and ***n*c**. This difference can be explained by the degree of the π-conjugation in S_1 states: the A_π value of ***n*b** is assumed to be smaller than those of ***n*a** and ***n*c**. Therefore, it is suggested

TABLE 3. Electrochemical Properties of bPEBs in CH_3CN and Annihilation Enthalpy Changes ($-\Delta H°$), E_{S1}, and ($-\Delta H° - E_{S1}$) of bPEBs in Bz

	in CH_3CN		in Bz		
bPEB	E_{ox} (V)	E_{red} (V)	$-\Delta H°$ (eV)	E_{S1} (eV)	$-\Delta H° - E_{S1}$ (eV)
1a	1.38[a]	−2.35[a]	3.92	3.54	+0.38
1b	1.65	−2.52	4.36	3.97	+0.39
1c	1.69	−2.38	4.26	3.68	+0.58
2a	1.45	−2.30	3.94	3.54	+0.40
2b	1.62	−2.52	4.33	3.97	+0.36
2c	1.56	−2.37	4.10	3.67	+0.43
3a	1.25	−2.35	3.79	3.46	+0.33
3b	1.32	−2.48	3.99	3.88	+0.11
3c	1.33	−2.39	3.91	3.56	+0.35
4a	1.57	−2.17	3.93	3.44	+0.49
4b	1.74	−2.36	4.29	3.82	+0.47
4c	1.69	−2.22	4.10	3.54	+0.56
5a	*b*	*b*		3.37	
5b	1.63	−2.39	4.21	3.82	+0.39
5c	1.60	−2.28	4.07	3.46	+0.61
6a	1.27	−2.24	3.70	3.33	+0.37
6b	1.32	−2.39	3.90	3.76	+0.14
6c	1.34	−2.28	3.81	3.36	+0.45
7a	0.60	−2.26	3.05	2.94	+0.11
7b	0.60	−2.36	3.15	3.14	+0.01
7c	0.59	−2.28	3.06	2.88	+0.18

[a] Reference 21. [b] Not dissolved in the solvent.

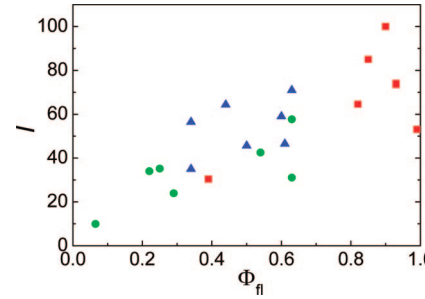

FIGURE 4. Plots of I value versus Φ_{fl} for ***n*a** (red square), ***n*b** (green circle), and ***n*c** (blue triangle) in Bz.

(20) Gross, E. M.; Anderson, J. D.; Slaterbeck, A. F.; Thayumanavan, S.; Barlow, S.; Zhang, S. R; Marder, H. K; Hall, M. F.; Nabor, J.-F; Wang, E. A; Mash, N. R; Armstrong, R. M.; Wightman, Y. *J. Am. Chem. Soc.* **2000**, *122*, 4972.

(21) Kilsa, K.; Kajanus, J.; Macpherson, A. N.; Martensson, J.; Albinsson, B. *J. Am. Chem. Soc.* **2001**, *123*, 3069.

SCHEME 3. Proposed Structure for the Formation of Donor-Acceptor-Type bPEBs in the S_1 and T_1 States during Pulse Radiolysis in Bz

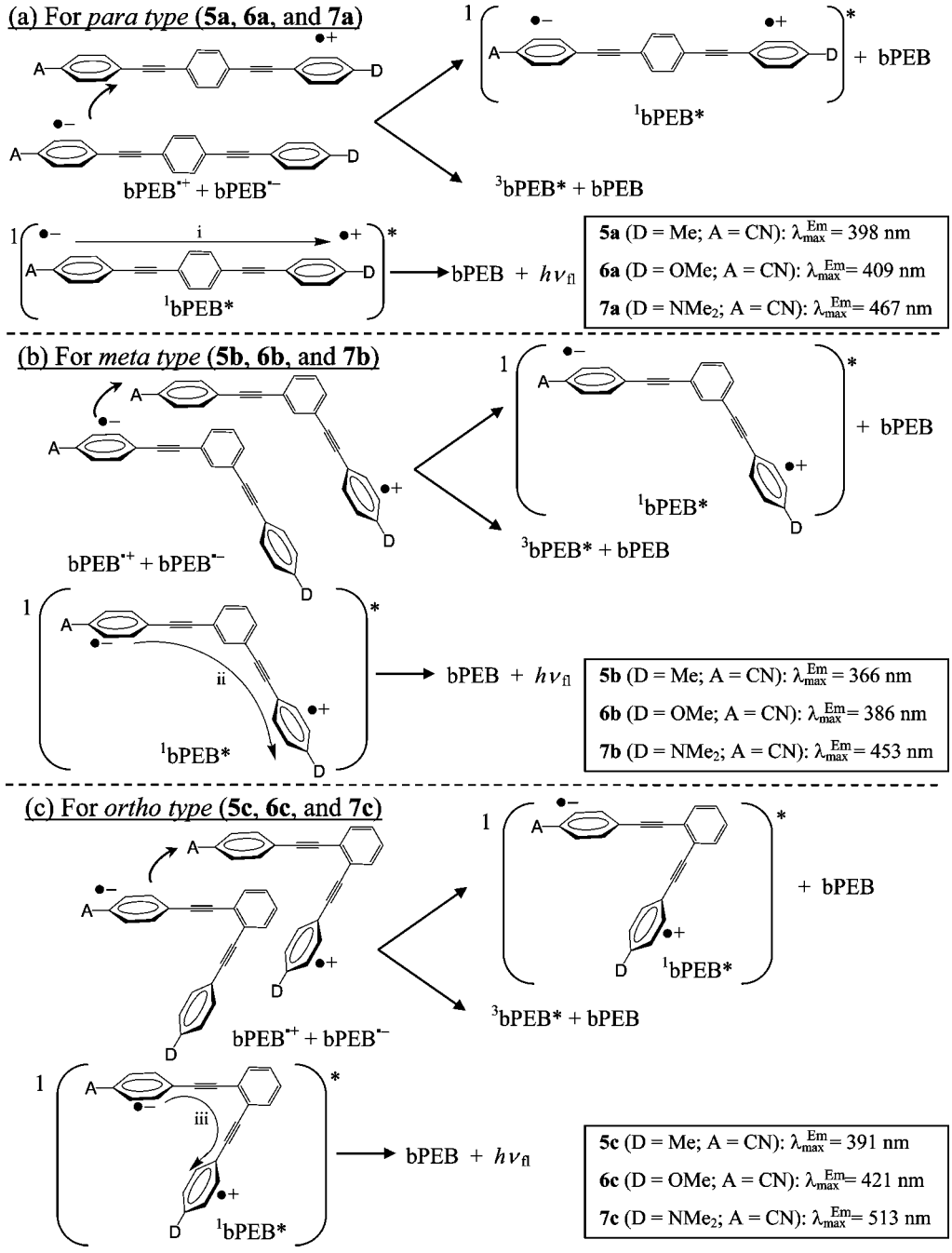

that the molecular design that extends the π-conjugation length is desirable in order to achieve the efficient charge recombination emission.

Conclusions

Through control of the substitution pattern of the regioisomeric electron donor- and/or acceptor-substituted bPEBs **1**−**7**, the fine-tuning of radiolysis-induced emission color and intensity can be achieved. Using pulse radiolysis technique, the charge recombination between $bPEB^{\bullet+}$ and $bPEB^{\bullet-}$ gives ^{1}bPEB* as the emissive species, which has the emission wavelengths 350−650 nm in the visible region. It is clearly indicated that the difference in the charge transfer conjugated pathways between donor and acceptor substituents, the linear- (path i), cross- (path ii), and bent-conjugated (path iii) pathways, strongly influence the HOMO−LUMO energy gap. In addition, our results show that the degree of the π-conjugation influences the luminescence intensity during pulse radiolysis. These specific emission properties of donor-acceptor-substituted bPEB may lead to customization of optical band gaps and luminescent efficiency for specialized materials applications.

Experimental Section

Solution Preparation. Benzene was purchased from Nacalai Tesque (spectral grade) and used as a solvent without further purification. All sample solutions were freshly prepared in 1 mM

concentration in Bz in a rectangular quartz cell (1.0 × 1.0 × 4.0 cm, path length of 1.0 cm). These solutions were saturated with Ar gas by bubbling for 10 min at room temperature before irradiation. All experiments were carried out at room temperature.

Measurements of Steady-State Spectral Properties. UV spectra were recorded in Bz with a Shimadzu UV-3100PC UV/vis spectrometer. Fluorescence spectra were measured by a Hitachi 850 spectrofluorometer. The fluorescence quantum yields (Φ_{fl}) were determined by using **1a** ($\Phi_{fl} = 0.90$ in cyclohexane, $\lambda_{ex} = 360$ nm)[22] standard.

Pulse Radiolysis. Pulse radiolysis experiments were performed using an electron pulse (28 MeV, 8 ns, 0.87 kGy per pulse) from a linear accelerator at Osaka University. The kinetic measurements were performed using a nanosecond photoreaction analyzer system (Unisoku, TSP-1000). The monitor light was obtained from a pulsed 450-W Xe arc lamp (Ushio, UXL-451−0), which was operated by a large current pulsed power supply that was synchronized with the electron pulse. The monitor light was passed through an iris with a diameter of 0.2 cm and sent into the sample solution at an intersection perpendicular to the electron pulse. The monitor light passing through the sample was focused on the entrance slit of a monochromator (Unisoku, MD200) and detected with a photomultiplier tube (Hamamatsu Photonics, R2949). The transient absorption and emission spectra were measured using a photodiode array (Hamamatsu Photonics, S3904-1024F) with a gated image intensifier (Hamamatsu Photonics, C2925−01) as a detector. All emission spectra were corrected for the spectral sensitivity of the apparatus. To avoid pyrolysis of the sample solution by the monitor light, a suitable cutoff filter was used.

(22) Sciano, J. C. *Handbook of Organic Photochemistry*; CRC Press: Boca Raton, FL, 1989; Vol. l, p 231.

Measurements of Electrochemical Properties. Oxidation (E_{ox}) and reduction potentials (E_{red}) were measured by cyclic voltammetry (BAS, CV-50W) with platinum working and auxiliary electrodes and an Ag/Ag^+ reference electrode at a scan rate of 100 mV s^{-1}. Measurements were performed in dry AN containing approximately 1 mM of AHs and 0.1 M tetraethylammonium perchlorate.

Acknowledgment. We thank the members of the Radiation Laboratory of ISIR, Osaka University for running the linear accelerator. This work has been partly supported by a Grant-in-Aid for Scientific Research (Project 17105005, 19350069, Priority Research (477), and others) from the Ministry of Education, Culture, Sports, Science and Technology (MEXT) of the Japanese Government and the U.S. National Science Foundation (CHE-0718242). One of the authors (S.S.) expresses his thanks for a JSPS Research Fellowship for Young Scientists and the Global COE Program "Global Education and Research Center for Bio-Environmental Chemistry" of Osaka University. T.R. thanks the Lundbeck Foundation for a fellowship during his time at Oregon.

Note Added after ASAP Publication. An additional acknowledgment was added in the version published May 8, 2009.

Supporting Information Available: Experimental details for all new compounds and copies of ^1H and ^{13}C NMR spectra. This material is available free of charge via the Internet at http://pubs.acs.org.

JO900494J